proceedings

MDPI

Proceedings

Direct Contacting of 2D Nanosheets by Metallic Nanoprobes †

F. Giubileo [1,*], F. Urban [1,2], A. Grillo [1,2], A. Pelella [1,2], E. Faella [2] and A. Di Bartolomeo [1,2]

[1] CNR-SPIN Salerno Via Giovanni Paolo II 132, 84084 Fisciano, Salerno, Italy; furban@unisa.it (F.U.); agrillo@unisa.it (A.G.); apelella@unisa.it (A.P.); adibartolomeo@unisa.it (D.B.)

[2] Physics Department "E. R. Caianiello", University of Salerno, Via Giovanni Paolo II 132, 84084 Fisciano, Salerno, Italy; efaella@unisa.it

* Correspondence: filippo.giubileo@spin.cnr.it

† Presented at the 2nd International Online-Conference on Nanomaterials, 15–30 November 2020; Available online: https://iocn2020.sciforum.net/.

Published: 15 November 2020

Abstract: We present a simple and fast methodology to realize metal contacts on two-dimensional nanosheets. In particular, we perform a complete characterization of the transport properties of MoS_2 monolayer flakes on SiO_2/Si substrates by using nano-manipulated metallic tips as metallic electrodes directly approached on the flake surface. We report detailed experimental investigation of transport properties and contact resistance in back-gated field effect transistor in which the Si substrate is used as the gate electrode. Moreover, profiting of the n-type conduction as well as the high aspect ratio at the edge of the MoS_2 flakes, we also explored the possibility to exploit the material as field emitter. Indeed, by retracting one of the metallic probes (the anode) from the sample surface, it has been possible to switch-on a field emitted current by applying a relative low external electric field of few tens of Volts for cathode-anode separation distance below 1 μm. Experimental data are then analysed in the framework of Fowler-Nordheim theory and its extension to the two-dimensional limit.

Keywords: two-dimensional materials; transition metal dichalcogenides; molybdenum disulfide; field-effect transistor; transport properties; field emission

1. Introduction

Molybdenum disulfide (MoS_2) is one of the most investigated transition-metal dichalcogenides (TMDs) for exploitation in next-generation two-dimensional (2D) devices, including field-effect transistors [1–4], solar cells [5], photodetectors [6,7], field emission devices [8–11], chemical or biological sensors [12,13], etc.

MoS_2 has a crystal structure characterized by a hexagonal layer of Mo atoms between two layers of S atoms. Layers are bonded together by van der Waals forces. MoS_2 flakes can be fabricated either by mechanical exfoliation or chemical vapor deposition [14]. Bulk MoS_2 has 1.2 eV indirect bandgap, while mono-layer (1 L) and bilayer (2 L) MoS_2 have 1.8 eV and 1.6 eV indirect bandgap, respectively [15]. Consequently, both 1 L and 2 L MoS_2 can be used to realize field-effect transistors with high On/Off ratio and photoresponse [16]. On the other hand, carrier mobility is typically limited to few-tens $cm^2\ V^{-1}\ s^{-1}$. Moreover, ohmic contacts (with low resistance) are crucial to improve device performance [17].

In this paper, we demonstrate a simple method to realize electrical contacts on MoS_2 flakes by using nanomanipulated metallic probes inside a scanning electron microscope (SEM). We show that this technique allows complete characterization of the back-gated field-effect transistor (FET) as well as to check the field emission properties of the MoS_2 flake.

2. Materials and Methods

The MoS_2 flakes studied in this work have been grown on Si/SiO_2 substrates by means of chemical vapour deposition technique in which S powder and a saturated ammonium heptamolybdate solution have been used as precursors. Few-layer MoS_2 flakes have been characterized by micro-Raman spectroscopy (λ = 532 nm). The experimental setup for electrical characterization is realized inside a SEM chamber (see Figure 1a) provided with two piezo-driven nano-manipulators for precise positioning (step resolution ~5 nm) of metallic probes (tungsten tips). A semiconductor parameter analyser (Keithley 4200-SCS) is then used as source-measurement unit, to apply bias up to ±100 V and to measure current with resolution better than 0.1 pA. Electrical measurements are performed at room temperature and in high vacuum (10^{-6} mbar) after gently approaching the tungsten tips on the MoS_2 flake (a real image taken inside the SEM chamber is shown in Figure 1b), and using the Si substrate as back gate.

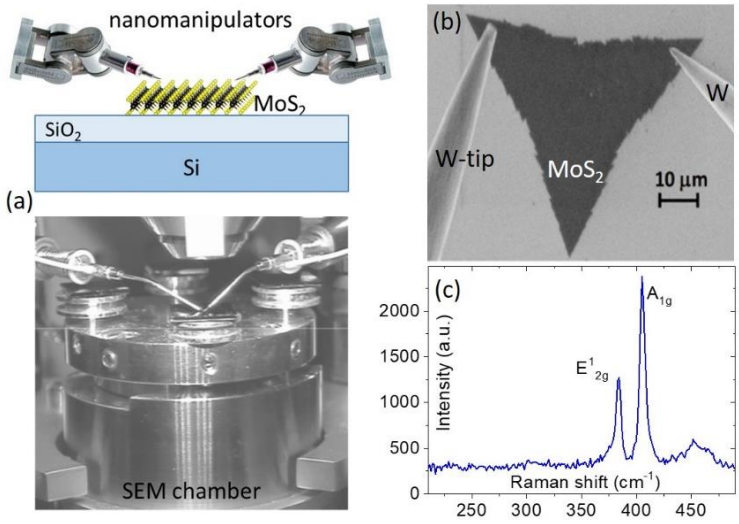

Figure 1. (**a**) Schematic and real image of the nanomanipulators contacting the MoS_2 flake, inside the SEM chamber. (**b**) SEM image of a contacted MoS_2 flake. (**c**) Raman spectrum of MoS_2 flake.

The micro-Raman analysis of the MoS_2 flake has shown a spectrum (see Figure 1c) with two peaks corresponding to the E^1_{2g} and A_{1g} modes, separated of about 20 cm^{-1}, giving indication that the sample under investigation is a monolayer.

3. Results and Discussion

In Figure 2a we report the output characteristics ($I_{ds} - V_{ds}$) measured in the range ±0.5 V for different values of the gate voltage (V_{gs}). We notice a slight rectification that can be explained as the result of asymmetric Schottky barriers forming at the tungsten/MoS2 interfaces [18]. By varying the distance between the two tungsten tips, we can modulate the channel length of the FET, thus realizing an experiment based on the Transfer Length Method (TLM) [19] to evaluate the contact resistance at the tungsten/MoS_2 interface. In Figure 2b we show the measured total resistance R_{tot} versus d, with $R_{tot} = 2R_c + \frac{R_s}{W}d$, where R_c is the contact resistance, R_s is the MoS2 sheet resistance, W is the channel width (assumed equal to the tip diameter, 200 nm), d is the channel length, i.e. the separation between the two tips. [24,25] Experimental data have linear behavior, from which specific area contact resistivity and sheet resistance can be evaluated as $\rho_c \approx 4 \times 10^{-2}\ \Omega cm^2$ and $R_s \approx 10^8\ \Omega/\square$ from the intercept the slope of the linear fit, respectively.

The transfer characteristics ($I_{ds} - V_{gs}$) reported in Figure 2c have been measured for different gate voltage ranges up to ±60 V, with $V_{ds} = -5$ V, and by positioning the tungsten tips at separation of 13 µm. The device has n-type behavior, with threshold voltage of about -10 V, and it can be explained in terms of chemisorption of oxygen on MoS_2 or sulphur vacancies [20–22].

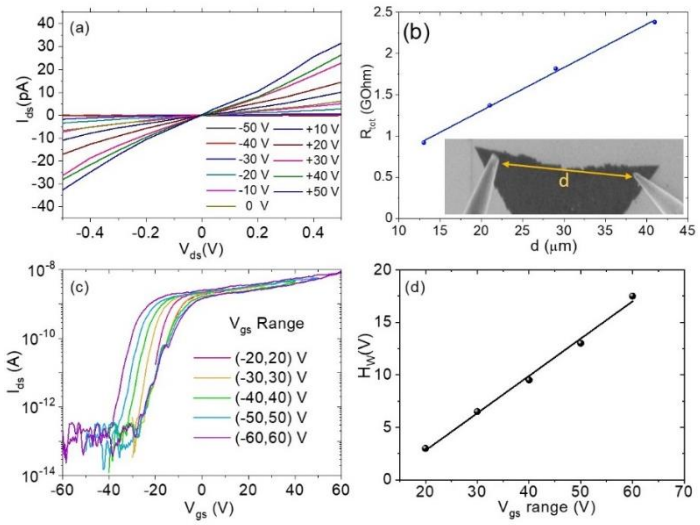

Figure 2. (**a**) Output characteristics ($I_{ds} - V_{ds}$) measured for different gate voltage values. (**b**) R_{tot} vs d plot and linear fit. The inset show how d is measured. (**c**) Transfer characteristics ($I_{ds} - V_{gs}$) measured for different gate voltage ranges. (**d**) Linear dependence of the hysteresis width Hw as function of V_{gs}.

From the transfer characteristic measured in the range ±50 V we have estimated the on/off ratio ~10^5, a subthreshold swing $SS \approx 4\ \frac{V}{decade}$, and a mobility $\mu = 1\ \mathrm{cm^2\,V^{-1}\,s^{-1}}$, a value within the typical range ($0.02 - 100\ \mathrm{cm^2\,V^{-1}\,s^{-1}}$) reported for MoS_2 based FETs on SiO_2 [23,24]. The low mobility can be attributed to the high contact resistance and to high defects or traps density [25].

In Figure 3c, we show the transfer characteristics measured by sweeping the gate voltage different ranges, from ±20 V up to ±60 V. The curves have a clear hysteresis that we explain as due to negative charge trapping [20]. We observe that the the hysteresis width (H_W), estimated at $I_{ds} = 0.1$ nA, has a linear dependence on the V_{gs} sweeping range (See Figure 3d). This behavior can be ascribed to the trapping process driven by the gate voltage and the effects on the MoS_2/Si-substrate capacitor.

Finally, we also investigated the field emission (FE) properties of the MoS_2 flake, profiting of the n-type conduction and the high aspect ratio of the flake side. By retracting the tip-anode at a distance h = 900 nm from the MoS_2 edge, we can measure the current emitted from the flake under the application of an external electric field (Figure 3a). More precisely, we applied a voltage bias up to 120 V on the anode and we measured the current emitted from the flake (cathode) with a resolution better that 0.1 pA. The current–voltage ($I_{ds} - V_{ds}$) curves have been measured at fixed cathode-anode separation h, and for two different values of gate voltage.

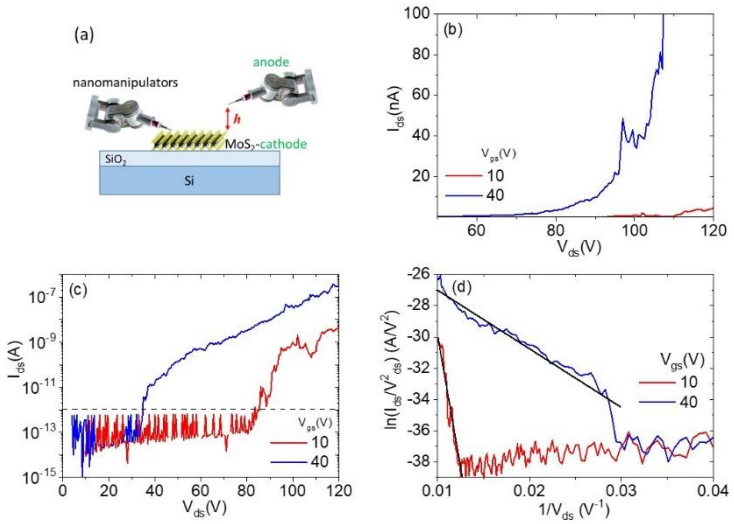

Figure 3. (**a**) Schematic of field emission setup. (**b**) $I_{ds} - V_{ds}$ field emission curves, on linear scale, measured for two different gate voltages. (**c**) Same $I_{ds} - V_{ds}$ field emission curves, reported on logarithmic scale. (**d**) Fowler-Nordheim plots and linear fittings.

The FE characteristics have been measured by applyng a bias voltage on the anode up to +120 V, by keeping a fixed gate voltage of 10 V and 40 V, respectively. The measured curves are reported on linear scale (Figure 3b) and on logarithmic scale (Figure 3c). Interestingly, we observe that the FE current is larger for $V_{gs} = 40$ V suggesting that the gate voltage increases the n-doping of the MoS_2 flake [26].

We analyzed the FE curves in the framework of Fowler-Nordheim (FN) theory [27] for which the FE current is expressed as

$$I_{ds} = A\frac{(\beta V_{ds}/h)^2}{\Phi} S \cdot exp\left(-B\frac{\Phi^{\frac{3}{2}}}{(\beta V_{ds}/h)}\right), \quad (1)$$

where $A = 1.54 \times 10^{-6}\ \mathrm{A\,V^{-2}\,eV}$ and $B = 6.83 \times 10^{7}\ \mathrm{V\,cm^{-1}\,eV^{-3/2}}$, Φ is the work function of the emitter, S is the emitting surface area, and β is the field enhancement factor. Accordingly, for FE curves it is expected that $ln(I_{ds}/V_{ds}^{2})$ versus $1/V$ is linear (FN plot), and β can be evaluated from its slope.

In Figure 5d, we report the FN plots that demonstrate the FE nature of the measured current. For $V_{gs} = 40$ V, we found a turn-on field $E_{on} = 40\ \mathrm{V\,\mu m^{-1}}$, (defined as the field to obtain a FE current of 1 pA) and $\beta \approx 200$.

4. Conclusions

We demonstrate a simple and fast methodology to realize metal contacts on two-dimensional nanosheets by gently approaching nanomanipulated tungsten tips inside a scanning electron microscope. We contacted a MoS_2 monolayer to form a back-gated FET, and we performed complete electrical characterization, reporting specific area contact resistivity of $4 \times 10^{-2}\ \Omega\,\mathrm{cm^2}$, sheet resistance of $10^8\ \Omega/\square$, on/off ratio of 10^5, subthreshold swing of 4 V/decade, and mobility of $1\ \mathrm{cm^2\,V^{-1}\,s^{-1}}$. Finally, by retracting the tip-anode we performed field emission characterization of the MoS_2 flake, reporting that the FE current can be modulated by the gate bias.

Conflicts of Interest: The authors declare no conflict of interest.

References

1. Tong, X.; Ashalley, E.; Lin, F.; Li, H.; Wang, Z.M. Advances in MoS2-Based Field Effect Transistors (FETs). *Nano-Micro Lett.* **2015**, *7*, 203–218, doi:10.1007/s40820-015-0034-8.
2. Seo, D.; Lee, D.Y.; Kwon, J.; Lee, J.J.; Taniguchi, T.; Watanabe, K.; Lee, G.-H.; Kim, K.S.; Hone, J.; Kim, Y.D.; et al. High-performance monolayer MoS2 field-effect transistor with large-scale nitrogen-doped graphene electrodes for Ohmic contact. *Appl. Phys. Lett.* **2019**, *115*, 012104, doi:10.1063/1.5094682.
3. Di Bartolomeo, A.; Grillo, A.; Urban, F.; Iemmo, L.; Giubileo, F.; Luongo, G.; Amato, G.; Croin, L.; Sun, L.; Liang, S.-J.; et al. Asymmetric Schottky Contacts in Bilayer MoS 2 Field Effect Transistors. *Adv. Funct. Mater.* **2018**, *28*, 1800657, doi:10.1002/adfm.201800657.
4. Divya Bharathi, N.; Sivasankaran, K. Research progress and challenges of two dimensional MoS2 field effect transistors. *J. Semicond.* **2018**, *39*, 104002, doi:10.1088/1674-4926/39/10/104002.
5. Hao, L.; Liu, Y.; Gao, W.; Han, Z.; Xue, Q.; Zeng, H.; Wu, Z.; Zhu, J.; Zhang, W. Electrical and photovoltaic characteristics of MoS 2 /Si *p-n* junctions. *J. Appl. Phys.* **2015**, *117*, 114502, doi:10.1063/1.4915951.
6. Lopez-Sanchez, O.; Lembke, D.; Kayci, M.; Radenovic, A.; Kis, A. Ultrasensitive photodetectors based on monolayer MoS2. *Nat. Nanotechnol.* **2013**, *8*, 497–501, doi:10.1038/nnano.2013.100.
7. Di Bartolomeo, A.; Genovese, L.; Foller, T.; Giubileo, F.; Luongo, G.; Croin, L.; Liang, S.-J.; Ang, L.K.; Schleberger, M. Electrical transport and persistent photoconductivity in monolayer MoS 2 phototransistors. *Nanotechnology* **2017**, *28*, 214002, doi:10.1088/1361-6528/aa6d98.
8. Fu, H.; Yu, K.; Li, H.; Li, J.; Guo, B.; Tan, Y.; Song, C.; Zhu, Z. Enhanced field emission and photocatalytic performance of MoS 2 titania nanoheterojunctions via two synthetic approaches. *Dalton Trans.* **2015**, *44*, 1664–1672, doi:10.1039/C4DT03035D.

9. Kashid, R.V.; Late, D.J.; Chou, S.S.; Huang, Y.-K.; De, M.; Joag, D.S.; More, M.A.; Dravid, V.P. Enhanced Field-Emission Behavior of Layered MoS_2 Sheets. *Small* **2013**, *9*, 2730–2734, doi:10.1002/smll.201300002.
10. Giubileo, F.; Grillo, A.; Passacantando, M.; Urban, F.; Iemmo, L.; Luongo, G.; Pelella, A.; Loveridge, M.; Lozzi, L.; Di Bartolomeo, A. Field Emission Characterization of MoS2 Nanoflowers. *Nanomaterials* **2019**, *9*, 717, doi:10.3390/nano9050717.
11. Giubileo, F.; Iemmo, L.; Passacantando, M.; Urban, F.; Luongo, G.; Sun, L.; Amato, G.; Enrico, E.; Di Bartolomeo, A. Effect of Electron Irradiation on the Transport and Field Emission Properties of Few-Layer MoS 2 Field-Effect Transistors. *J. Phys. Chem. C* **2019**, *123*, 1454–1461, doi:10.1021/acs.jpcc.8b09089.
12. Li, P.; Zhang, D.; Sun, Y.; Chang, H.; Liu, J.; Yin, N. Towards intrinsic MoS 2 devices for high performance arsenite sensing. *Appl. Phys. Lett.* **2016**, *109*, 063110, doi:10.1063/1.4960967.
13. Yan, L.; Shi, H.; Sui, X.; Deng, Z.; Gao, L. MoS 2 -DNA and MoS 2 based sensors. *RSC Adv.* **2017**, *7*, 23573–23582, doi:10.1039/C7RA02649H.
14. Sun, J.; Li, X.; Guo, W.; Zhao, M.; Fan, X.; Dong, Y.; Xu, C.; Deng, J.; Fu, Y. Synthesis Methods of Two-Dimensional MoS2: A Brief Review. *Crystals* **2017**, *7*, 198, doi:10.3390/cryst7070198.
15. Mak, K.F.; Lee, C.; Hone, J.; Shan, J.; Heinz, T.F. Atomically Thin MoS 2: A New Direct-Gap Semiconductor. *Phys. Rev. Lett.* **2010**, *105*, doi:10.1103/PhysRevLett.105.136805.
16. Lee, Y.T.; Kang, J.-H.; Kwak, K.; Ahn, J.; Choi, H.T.; Ju, B.-K.; Shokouh, S.H.; Im, S.; Park, M.-C.; Hwang, D.K. High-Performance 2D MoS2 Phototransistor for Photo Logic Gate and Image Sensor. *ACS Photonics* **2018**, *5*, 4745–4750, doi:10.1021/acsphotonics.8b01049.
17. Giubileo, F.; Di Bartolomeo, A. The role of contact resistance in graphene field-effect devices. *Prog. Surf. Sci.* **2017**, *92*, 143–175, doi:10.1016/j.progsurf.2017.05.002.
18. Di Bartolomeo, A.; Grillo, A.; Urban, F.; Iemmo, L.; Giubileo, F.; Luongo, G.; Amato, G.; Croin, L.; Sun, L.; Liang, S.-J.; et al. Asymmetric Schottky Contacts in Bilayer MoS 2 Field Effect Transistors. *Adv. Funct. Mater.* **2018**, *28*, 1800657, doi:10.1002/adfm.201800657.
19. Urban, F.; Lupina, G.; Grillo, A.; Martucciello, N.; Di Bartolomeo, A. Temperature and gate effects on contact resistance and mobility in graphene transistors by TLM and Y-function methods. *arXiv* **2019**, arXiv:1912.04623.
20. Di Bartolomeo, A.; Genovese, L.; Giubileo, F.; Iemmo, L.; Luongo, G.; Foller, T.; Schleberger, M. Hysteresis in the transfer characteristics of MoS 2 transistors. *2D Mater.* **2017**, *5*, 015014, doi:10.1088/2053-1583/aa91a7.
21. Qi, L.; Wang, Y.; Shen, L.; Wu, Y. Chemisorption-induced *n* -doping of MoS 2 by oxygen. *Appl. Phys. Lett.* **2016**, *108*, 063103, doi:10.1063/1.4941551.
22. Cho, K.; Kim, T.-Y.; Park, W.; Park, J.; Kim, D.; Jang, J.; Jeong, H.; Hong, S.; Lee, T. Gate-bias stress-dependent photoconductive characteristics of multi-layer MoS 2 field-effect transistors. *Nanotechnology* **2014**, *25*, 155201, doi:10.1088/0957-4484/25/15/155201.
23. Bao, W.; Cai, X.; Kim, D.; Sridhara, K.; Fuhrer, M.S. High mobility ambipolar MoS 2 field-effect transistors: Substrate and dielectric effects. *Appl. Phys. Lett.* **2013**, *102*, 042104, doi:10.1063/1.4789365.
24. Radisavljevic, B.; Kis, A. Mobility engineering and a metal–insulator transition in monolayer MoS2. *Nat. Mater.* **2013**, *12*, 815–820, doi:10.1038/nmat3687.
25. Urban, F.; Giubileo, F.; Grillo, A.; Iemmo, L.; Luongo, G.; Passacantando, M.; Foller, T.; Madauß, L.; Pollmann, E.; Geller, M.P.; et al. Gas dependent hysteresis in MoS 2 field effect transistors. *2D Mater.* **2019**, *6*, 045049, doi:10.1088/2053-1583/ab4020.
26. Di Bartolomeo, A.; Urban, F.; Passacantando, M.; McEvoy, N.; Peters, L.; Iemmo, L.; Luongo, G.; Romeo, F.; Giubileo, F. A WSe 2 vertical field emission transistor. *Nanoscale* **2019**, *11*, 1538–1548, doi:10.1039/C8NR09068H.
27. Fowler, R.H.; Nordheim, L. Electron Emission in Intense Electric Fields. *Proc. R. Soc. A Math. Phys. Eng. Sci.* **1928**, *119*, 173–181, doi:10.1098/rspa.1928.0091.